

Supporting Information

for

The Effect of the Donor Moiety of DPP Based Polymers on the Performance of Organic Electrochemical Transistors

Yazhou Wang[#], Amer Hamidi-Sakr[#], Jokubas Surgailis[#], Yecheng Zhou, Hailiang Liao, Junxin Chen, Genming Zhu, Zhengke Li, Sahika Inal^{*}, Wan Yue^{*}

Dr. Y. Wang, Prof. Y. Zhou, H. Liao, J. Chen, G. Zhu, Prof. Z. Li, Prof. W. Yue, State Key Laboratory of Optoelectronic Materials and Technologies, Key Laboratory for Polymeric Composite and Functional Materials of Ministry of Education, Guangzhou Key Laboratory of Flexible Electronic Materials and Wearable Devices, School of Materials and Engineering, Sun Yat-Sen University, Guangzhou 510275, China.

Dr. A. Hamidi-Sakr, J. Surgailis, Prof. S. Inal, King Abdullah University of Science and Technology (KAUST), Biological and Environmental Science and Engineering Division, Organic Bioelectronics Laboratory, Thuwal 23955-6900, Saudi Arabia.

Contents

1. Materials and methods.....	S2
2. Molecular weights of the polymers.....	S5
3. Thermogravimetric analysis (TGA).....	S5
4. Absorption spectra.....	S6
5. DFT.....	S6
6. Cyclic voltammetry	S8
7. OECT Stability and Transient Response.....	S9
8. Electrochemical impedance spectroscopy (EIS).....	S10
9. Electrochemical quartz crystal microbalance (EQCM-D).....	S11
10. Tables of important parameters.....	S11
11. Synthesis of monomers and polymers	S12
12. NMR	S17
13. References.....	S25

1. Materials and Methods

Materials: Solvents for spectroscopic studies were of spectroscopic grade, purchased from Sigma Aldrich, and used as received. The monomers were purified by column chromatography using silica gel (General-Regent, 200-300 mesh) or GPC (Gel Permeation Chromatography Agilent1260 Infinity II), the polymers are purified by Soxhlet extraction. ^1H and ^{13}C NMR spectra were recorded in CDCl_3 or 1,1,2,2-Tetrachloroethane- d_2 (TCE- D_2) with a 400 HMZ or 500 HMz Bruker Avance III spectrometer.

Absorption spectra of polymers in solution: Absorption spectra were measured using Agilent Technologies (Cary 5000/6000i) Cary Win UV-Vis spectrophotometer in a 1-cm quartz cell. The polymers were dissolved in chloroform at a concentration of 1.0×10^{-5} M.

Cyclic voltammetry for EA and IP determination: The measurements were carried out using a standard commercial electrochemical analyzer (Shanghai Chenhua Instrument co. LTD., CHI520E) with a three-electrode single-compartment cell equipped with an Ag/AgCl reference electrode and a Pt wire auxiliary electrode. Before the measurements, the polymers were drop casted on a glassy carbon, which was used as a working electrode. The measurements were carried out in acetonitrile (HPLC grade), which was dried over calcium hydride under argon and degassed. 0.1 M tetrabutylammonium hexafluorophosphate ($n\text{-Bu}_4\text{NPF}_6$, Shanghai Macklin Biochemical Co., Ltd) was used as the supporting electrolyte and ferrocene (Fc) as an internal standard.

Molecular weight determination: Matrix-assisted Laser Desorption/ionization time-of-flight (MALDI-TOF) mass spectra of the polymers were recorded using a Bruker Daltonik (solariX) mass spectrometer.

Thermogravimetric analysis (TGA): The measurements were conducted on a Netzsch STA 449F3 apparatus from 25 °C to 700 °C at a heating rate of 10 °C min^{-1} under a nitrogen atmosphere.

Atomic force microscopy (AFM): AFM measurements were performed in tapping mode, using Bruker dimension icon AFM with a silicon tip. The measurements were performed with films which were spin-coated on ITO substrates from a 5 mg. mL^{-1} chloroform solution. First, the AFM images of the pristine films were measured. The same films were immersed into 0.1 M NaCl for 1h, which were then taken back to the AFM chamber. These hydrated films were used as working electrodes in a CV set-up with 0.1 M NaCl as the electrolyte. After two CV cycles, they were washed with deionized water, dried with nitrogen, and analyzed by AFM.

Electrochemical quartz crystal microbalance with dissipation monitoring (EQCM-D): Measurements were performed using the QSense Analyzer, a QSense Electrochemistry Module (QEM 401) and gold with titanium adhesion layer sensors (QSensors QSX 338) from Biolin Scientific in aqueous electrolyte. The analyzer measured the shift and dissipation of the

1st, 3rd, 5th, 7th, 9th and 11th frequency harmonics which provide information about the changes in sample mass and softness. First, the bare sensors were measured in air and after introducing NaCl(aq) 0.1 M. The electrolyte resulted in a large shift in the QCM-D signals due to the change in media density inside the chamber, which needs to be taken into consideration when calculating polymer swelling. After acquiring QCM-D baseline signals in both dry and wet conditions, the measured sensor was coated with a polymer film and placed back into the analyzer. The QCM-D signals were recorded again in dry state and with electrolyte after making sure that the f and D signals are stabilized (i.e., $\Delta f < 0.1$ Hz / 5 min). Using the QSoft software function “stitch data” provided the difference between the f and D signals before and after the sensor was coated with a polymer film in both dry state and with electrolyte. This difference was used to calculate the film areal mass in dry and swollen states, using the Sauerbrey equation:

$$\frac{\Delta m}{A} = -\Delta f_n \frac{\rho_q V_q}{2f_0^2 n} \approx \frac{-\Delta f_n}{n} 17.9 \text{ ng/cm}^2 \quad (\text{Equation 1})$$

Where Δf_n is the frequency shift of the nth overtone, A is the sensor active area, ρ_q is the density of quartz, V_q is the shear wave velocity in quartz, f_0 is the fundamental frequency and n is the overtone number. Film thickness was calculated by dividing the calculated areal mass with film density.

EQCM-D was performed using an Autolab PGstat128N potentiostat coupled with a QSense electrochemistry module (QEM 401). The integrated three-electrode setup comprised a Ag/AgCl reference electrode, Pt counter electrode and the polymer-coated Au QSensor acting as the working electrode with an electrochemical active area of 0.7854 cm².

Physical modelling of the measured f and D signals was done based on observed film characteristics. Films exhibiting a low degree of swelling and little to no energy losses were considered “rigid” and modelled using the Sauerbrey equation.

Grazing-incidence wide-angle X-ray scattering (GIWAXS): Samples for X-ray scattering were spin-coated on native oxide, silicon wafer pieces using the protocol described below. The incidence angle α of the incident beam was set to 0.18° with a photon energy of 8 KeV.

Optical and Electrochemical Characterization:

Sample preparation

All polymer films (on ITO and OECTs) were spin-coated from a chloroform solution at a concentration of 5 mg/mL. The spinning speed was 1500 rpm and the acceleration was 300 rpm/s and the overall time was 120 s. Devices were stored in vacuum for 2 hours after casting. For the Electrochemical impedance spectroscopy (EIS) measurements, the polymers were spin-coated on gold electrodes with a surface area of 0.0025 cm².

OECT fabrication

The devices were fabricated according to the parylene-C lift-off method reported previously.^[S1] Standard glass slides were cleaned via sonication in an acetone and isopropyl alcohol solution and dried with N₂. Connection pads and interconnects were deposited through a lift-off process using photolithographic patterning of positive photoresist (S1813). A subsequent metal deposition via sputtering of Cr (10 nm) and of Au (120 nm) and metal lift-off using acetone defines the Au lines. A first layer of parylene C (2 μm), deposited together with a small amount of 3-(trimethoxysilyl)propyl methacrylate (A-174 Silane) to enhance adhesion, acts as an insulator to prevent disturbing capacitive effects at the metal liquid interface. Subsequently, an antiadhesive layer was spin-coated using a dilution of industrial cleaner (2 wt %, Micro-90), and a second parylene-C sacrificial layer (2 μm) is deposited. To define the contact pads and the channel of the OECT, a second photolithographic patterning step using a thick positive photoresist (5 μm, AZ9260) and AZ developer was used to protect the parylene-C layers from a subsequent plasma reactive ion etching step. After spin coating the polymer layers, the peeling of the parylene-C sacrificial layer defined the channel dimensions. The thickness of the channels was measured using a DEKTAK 150 stylus profilometer. The devices have planar dimensions of L=10 μm and W= 100 μm.

OECT characterization

OECTs were characterized using a dual-channel source-meter unit (NI-PXI) with custom-written control code in LabVIEW. All measurements were performed using an Ag/AgCl pellet (D = 2mm × H = 2 mm; Warner Instruments) as the gate electrode. The electrolyte was contained in a PDMS well mounted on top of the OECT channels, and the electrolyte volume was constant at 100 μL for all measurements.

Electrochemical characterization

Electrochemical measurements were performed was performed with a three-electrode configuration using a potentiostat (Metrohm Autolab) Cyclic voltammograms at ambient temperature were recorded in a three-electrode set-up using an Ag/AgCl reference electrode and a Pt foil counter electrode. EIS measurements were conducted to determine the electrochemical capacitance of the films. Measurements were performed in 0.1 M NaCl at a DC offset potential and a sinusoidal AC amplitude of 10 mV, spanning a frequency range from 10 kHz to 0.1 Hz. The R(RC) fits were generated using EC-Lab software V10.44. The Capacitance was also calculated the film capacitances also using the equation below:

$$C = \frac{1}{2\pi f \times |Img(Z)|} \quad (\text{Equation 2})$$

where C is the capacitance, f is the frequency, and $|Img(Z)|$ is the magnitude of the imaginary part of the impedance. The capacitance values were normalized by film volume to determine the volumetric capacitance (C^*).

Spectroelectrochemistry

Spectro electrochemical measurements were performed using UV-1601 UV-VIS Shimadzu UV-Vis spectrometer coupled with a Metrohm Autolab PGSTAT101 potentiostat in a three-electrode setup. The polymer was deposited on ITO-coated glass slides which acted as the working electrode. The films were placed in a MM Spectro-EFC, SMA 905, 1.75 mL with optical windows purchased from Redox.me. A Pt mesh was used as the counter electrode, an Ag/AgCl electrode as the reference electrode, both immersed in 0.1 M NaCl solution. A background measurement was taken with a clean bare ITO substrate. The indicated voltages were applied for 10 s until the current stabilized prior to measuring of the spectrum.

2. Molecular weights of the polymers

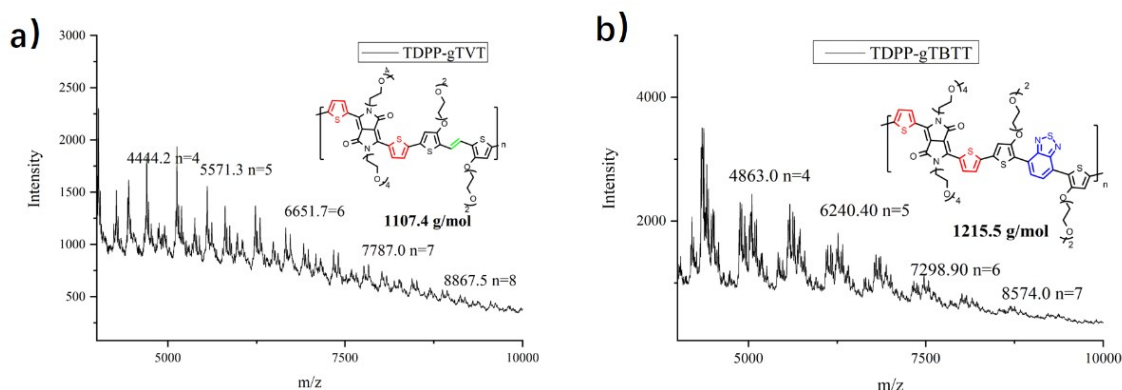


Figure S1. MALDI-TOF data for a) TDPP-gTVT and b) TDPP-gTBTT.

3. Thermogravimetric analysis (TGA)

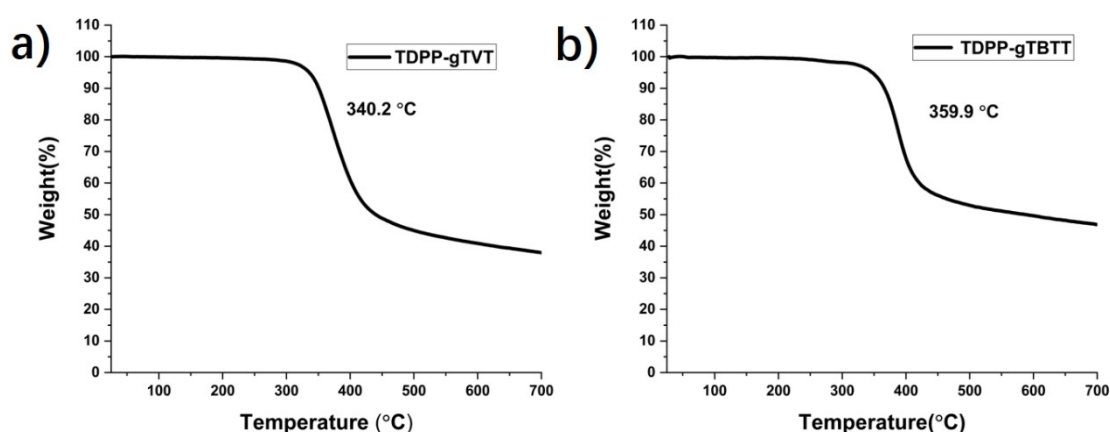


Figure S2. Thermogravimetric analysis curves of a) TDPP-gTVT and b) TDPP-gTBTT.

4. Absorption Spectra of Polymers

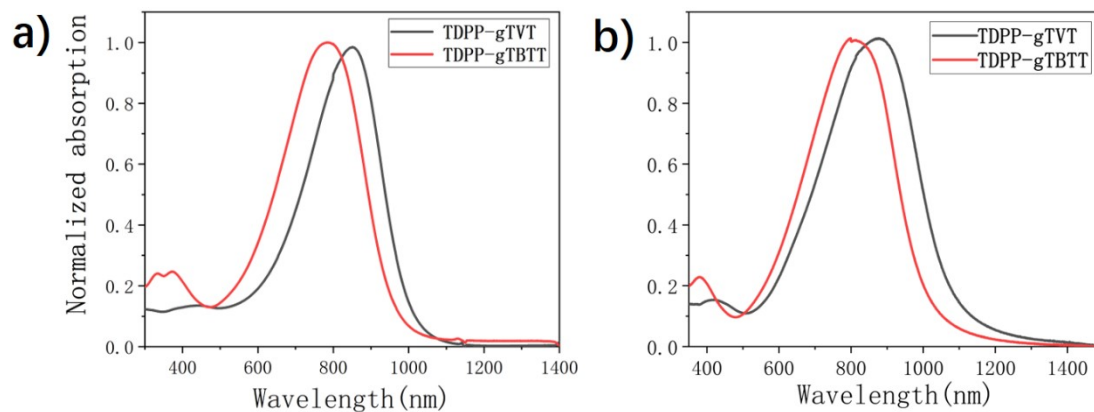
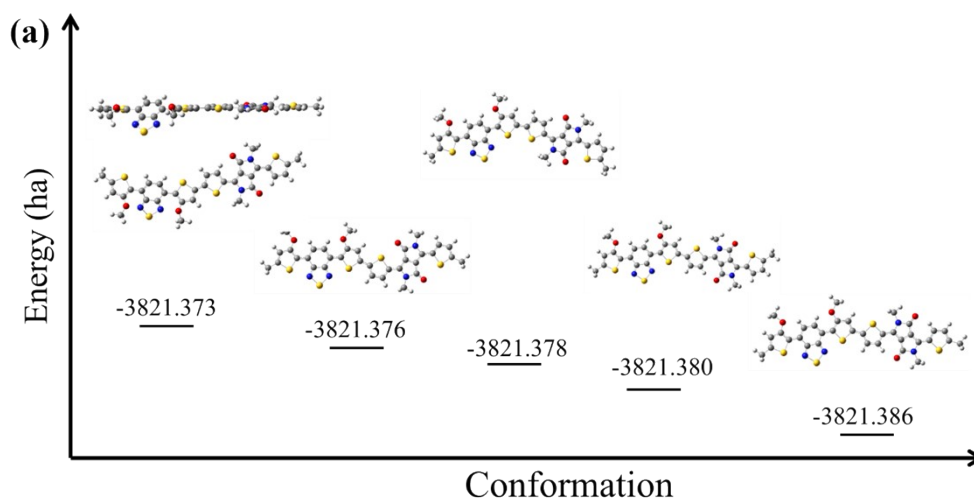


Figure S3. Normalized UV-Vis-NIR absorption spectra of the polymer solutions in chloroform at room temperature **(a)** and spin coated films from chloroform **(b)**.

5. Density Functional Theory (DFT) calculations

DFT calculations were performed by Gaussian 09. All molecular structures are optimized under the level of B3LYP/6-31G*. Configurations of these molecules were determined according to their optimized structures and energies. Figure S4 depicts the configuration difference highlighted in shallow blue, where the S atoms in two connected thiophene are on the same side or opposite sides. Configurations with lower energy were shown in Figure S4, which suggests that the S atoms in the neighboring thiophene prefer to arrange on opposite sides.



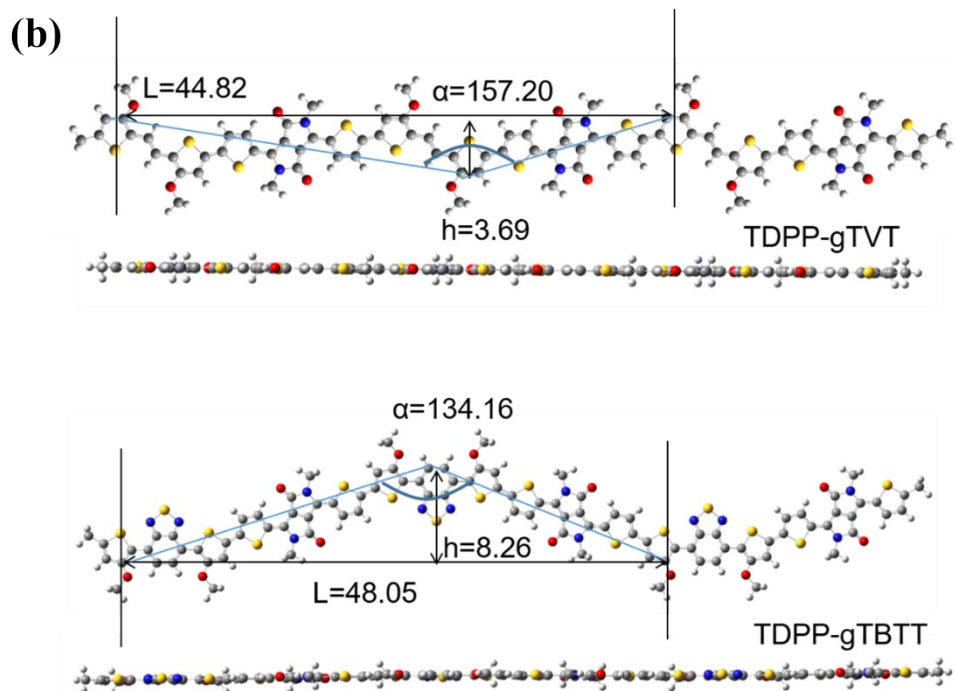


Figure S4. a) The energies of the conformations (the structures are fully optimized at the level of B3LYP/6-31G*), b) Top view and side view of geometry-optimized structures of the trimers. The extent of backbone curvature is depicted for each structure (highlighted in blue), along with the distance between the carbonyl of DPP and the oxygen of EG or sulfur of BT subunits.

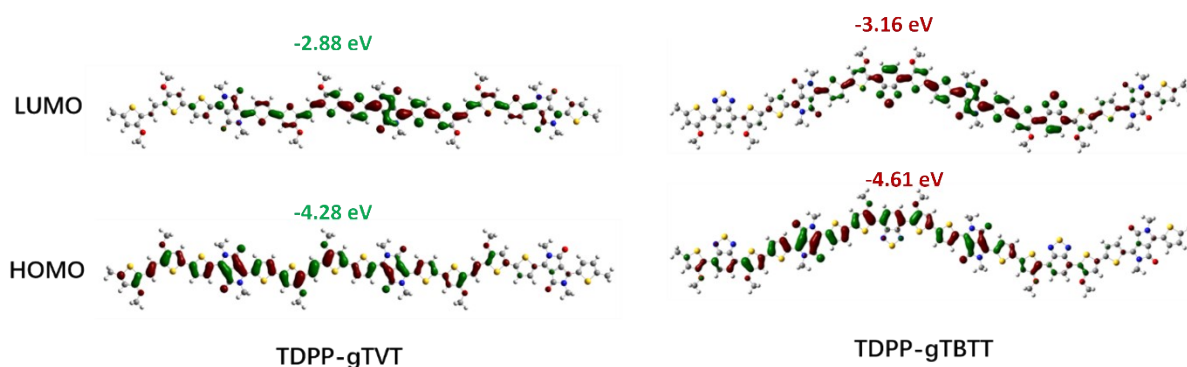


Figure S5. DFT-optimized molecular frontier orbitals of the trimers of TDPP-gTVT and TDPP-gTBTT.

6. Cyclic Voltammetry

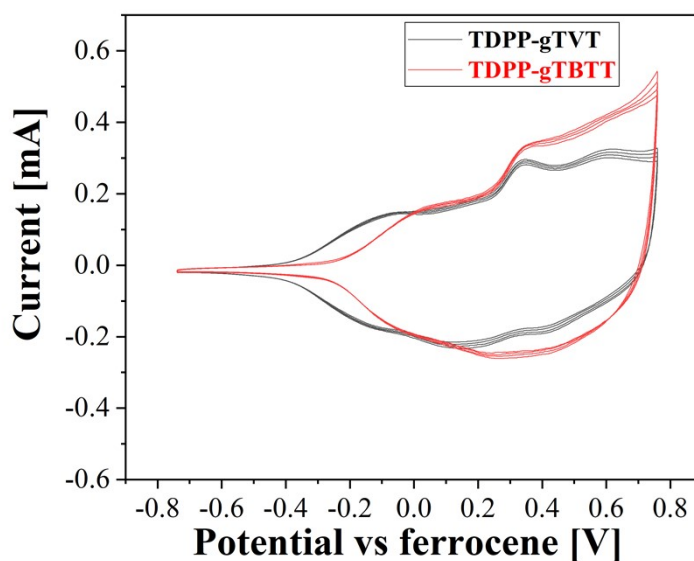


Figure S6. Four consecutive cyclic voltammetry scans of the polymer films drop-casted on ITO substrates. Measurements were acquired with a scan rate of 100 mVs^{-1} in 0.1 M tetrabutylammonium hexafluorophosphate (TBAPF_6) in acetonitrile. The onset of Fc/Fc^+ oxidation peak is 0.44 V .

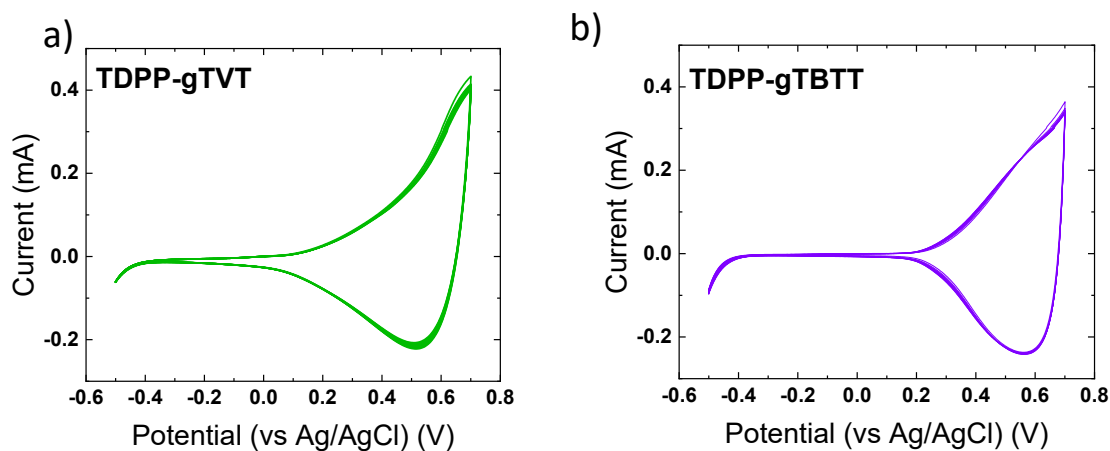


Figure S7. Cyclic voltammograms over 10 cycles acquired with a scan rate of 80 mV/s . The films were spin coated from chloroform on ITO over an area of 1 cm^2 .

7. OECT Stability and Transient Response

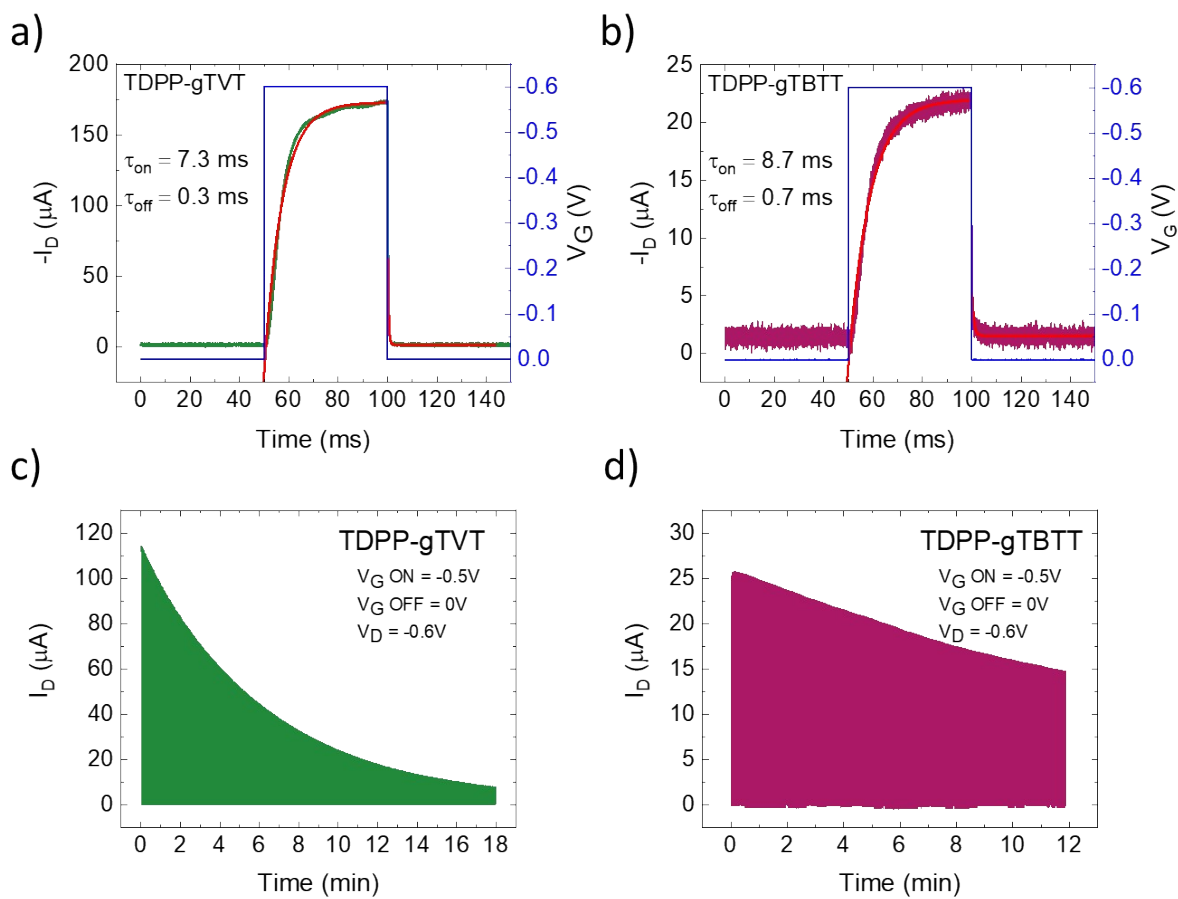


Figure S8. I_D response to an applied V_G pulse of -0.6 V for 50 ms **a)** TDPP-gTVT and **b)** TDPP-gTBTT; **c)** and **d)** show the OECT stability of TDPP-gTVT and TDPP-gTBTT, upon consecutive pulses at the gate electrode. Duty time is 1 sec.

8. Electrochemical Impedance Spectroscopy (EIS)

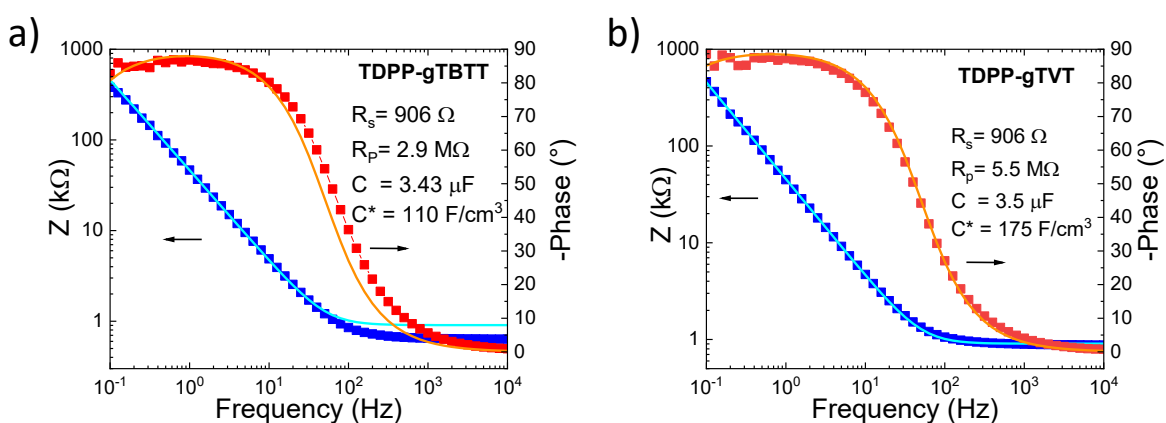


Figure S9. Electrochemical impedance spectra (Bode plots) of **a)** TDPP-gTVT and **b)** TDPP-gTBTT recorded at an offset bias (V_{offset}) ($V_{\text{offset}}=0.6$ V vs. Ag/AgCl). The modulus of the impedance, $|Z|$ (blue symbols), and phase (red symbols) are plotted as a function of frequency. The results fit $R_s(R_p||C)$ equivalent circuit where R_s is the electrolyte resistance, R_p and C

describe the polymer film's resistance and capacitance, respectively. Fits are shown as lines ($|Z|$ fit, cyan; phase fit, orange).

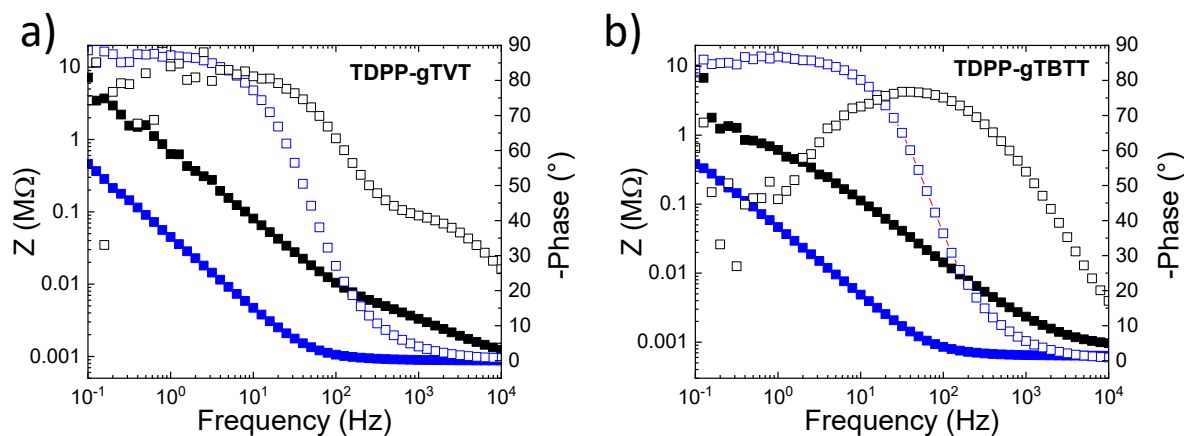


Figure S10. Electrochemical impedance spectra (Bode plots) of **a) TDPP-gTVT** and **b) TDPP-gTBTT**. The modulus of the impedance, $|Z|$ (full symbols), and phase (hollow symbols) are plotted as a function of frequency. An offset bias (V_{offset}) ($V_{\text{offset}}=0.6$ V vs. Ag/AgCl) was used to dope the films. The impedance data in doped state are represented in blue and the black symbols represent the impedance data at 0 V vs. Ag/AgCl.

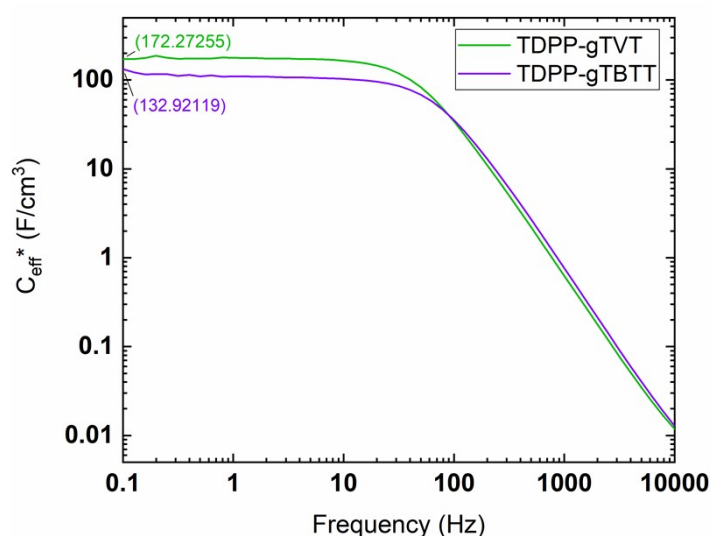


Figure S11. The effective volumetric capacitances of the polymers. Values shown are C^* calculated at $f = 0.1$ Hz.

9. EQCM-D

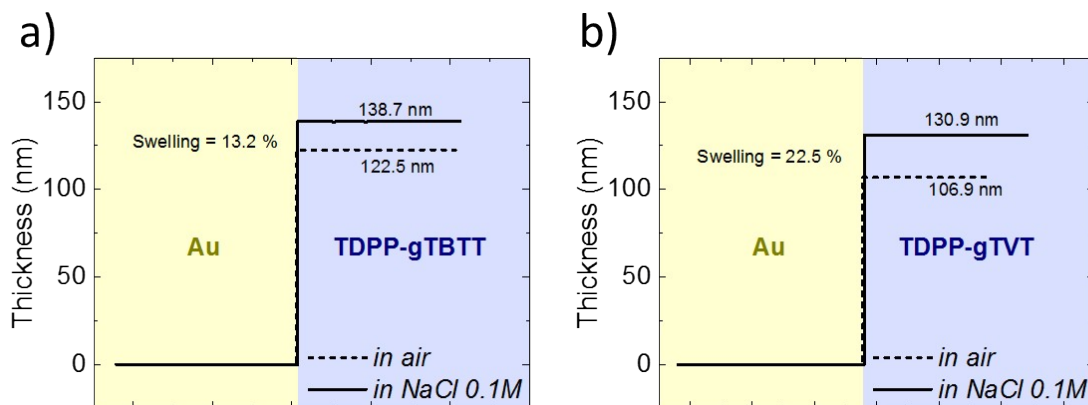


Figure S12. Thickness of a) TDPP-gTBTT and b) TDPP-gTVT films in dry state (dashed line) and after exposure to electrolyte (solid line).

10. Tables of important parameters

Table S1. Comparison of the OECT Performance of D-A Type Polymers

Polymers	μ^g [cm ² /V. s]	C^* [F/cm ³]	μC^{*f} [F /cm. V. s]	V_{TH} [V]	Reference
PIBET-AO ^b	-- ^a	-- ^a	5.4	-0.44	[S2]
CPEK ^c	5×10^{-3}	134	0.67	-- ^a	[S3]
P(gPyDPP-MeOT2) ^d	0.030	60	1.8	-- ^a	[S4]
p(gDPP-TT) ^d	0.57 ± 0.09	184	125 ± 22	-0.54	[S5]
p(gDPP-T2) ^d	1.55 ± 0.17	196	342 ± 35	-0.52	[S5]
p(gDPP-MeOT2) ^d	0.28 ± 0.04	169	57 ± 5	-0.26	[S5]
PDPP-DT ^e	2.50/1.21	224/123	$559 \pm 65 / 149 \pm 61$	-0.59/-0.93	[S6]
TDPP-gTVT^d	1.1	173.5 ± 5	205.2 ± 12	-0.36	this work
TDPP-gTBTT^d	0.18	122.5 ± 15	21.5 ± 0.7	-0.42	this work

^aData not available in the reference; Measurements were performed with channel geometries (W/L) of ^b 390000/20 μm , ^c 1000/40 μm , ^d 100/10 μm , and ^e 5/10 μm , ^f μC^* was estimated based on the given transconductance and device geometries. ^g μ was calculated from the measured μC^* and C^* .

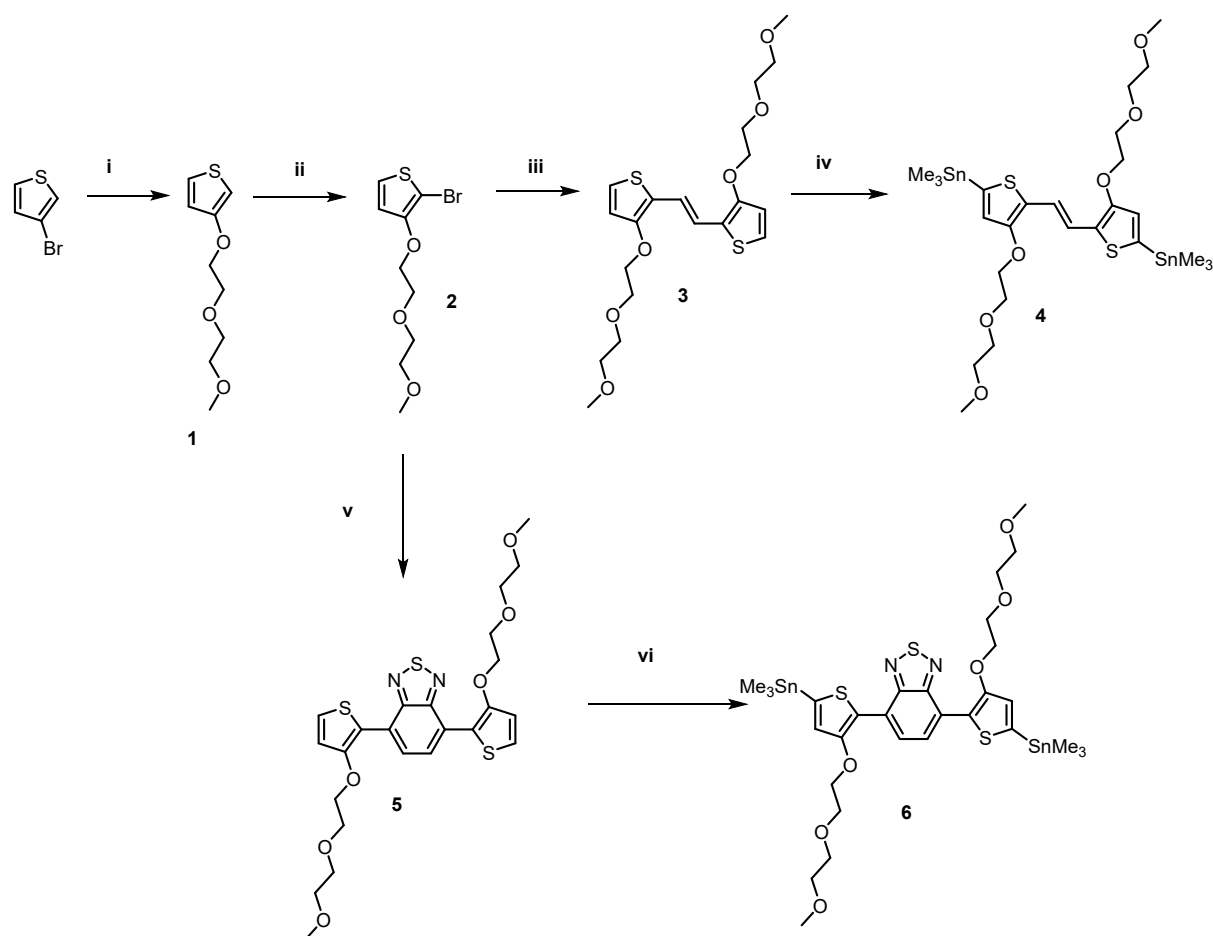
Table S2. Solid state packing parameters for the polymers.

	$q_{(100)}$ (\AA^{-1})	$d_{(100)}$ (\AA)	$q_{(010)}$ (\AA^{-1})	$d_{(010)}$ (\AA)	L_C (010) (\AA)	dominant texture
TDPP-gTVT in-plane	0.332	18.92	1.79	3.51	20.0	face-on
TDPP-gTVT out-of-plane	0.332	18.92	1.75	3.59	23.5	
TDPP-gTBTT in-plane	0.329	19.09	1.64	3.83	12.7	face-on
TDPP-gTBTT out-of-plane	-	-	1.73	3.63	20.2	

(010) peaks were fit with the summation of pseudo-Voigt distributions.

11. Synthesis of Monomers and Polymers

Scheme S1: Synthetic route of 1-6.



Reaction conditions: i) t-BuOK, 2-(2-Methoxyethoxy)ethanol, RT, then 100 °C; ii) NBS, THF/Hexane, 0 °C; iii) 2-Bis(tributylstannyl)ethene, Pd₂(dba)₃, P(o-tol)₃, 100 °C ; iv) n-BuLi, THF, -78 °C, SnClMe₃, then RT; v) 4,7-Bis(4,4,5,5-tetramethyl-1,3,2-dioxaborolan-2-yl)-2,1,3-benzothiadiazole, Pd₂(dba)₃, P(o-tol)₃, tricaprylylmethylammonium chloride, aq.K₃PO₄, toluene; vi) n-BuLi, THF, -78 °C, SnClMe₃, then RT.

1-6 were synthesized according to the literature. [S7-S12]

3: 2 (3.00 g, 10.67 mmol, 2.5 equiv.), Pd₂(dba)₃ (100 mg), and P(o-tol)₃ (200 mg) were added to round-bottom flask and degassed with N₂ for 3 times. Then 2-bis(tributylstannyl)ethene (2.60 g, 4.28 mmol, 1 equiv.) and 30 ml anhydrous toluene were added under N₂ and then stirred at 100 °C overnight. The solvent was removed under vacuum and purified by silica gel column chromatography to get 550 mg liquid **3** (30 %). ¹H NMR (400 MHz, 300K, CDCl₃) δ (ppm): 7.00 (d, *J* = 5.5 Hz, 2H), 6.97 (s, 2H), 6.78 (d, *J* = 5.5 Hz, 2H), 4.22 – 4.18 (m, 4H), 3.86 – 3.81 (m, 4H), 3.75 – 3.71 (m, 4H), 3.61 – 3.56 (m, 4H), 3.39 (s, 6H). ¹³C NMR (300 K, 101 MHz, CDCl₃) δ: 153.61, 122.22, 121.56, 118.06, 116.21, 72.01, 71.41, 70.87, 70.15, 69.95, 59.08.

4: Under N₂ flow, a dry 100 mL round bottom flask with magnetic stir bar was charged with 500 mg **3** (0.95 mmol) and 20 mL dry THF. The solution was cooled to -78 °C with an acetone/dry ice bath over 15 min, and then 1.49 mL (1.6 M) n-butyllithium (2.38 mmol) was added dropwise over 10 min. The reaction mixture was allowed to stir at -78 °C for two hours, warmed to room temperature for 15 min, and then cooled back down to -78 °C. 2.85 mL 1.0 M trimethyltin chloride in THF was added in one portion, and the reaction was stirred and allowed to warm to room temperature overnight. After quenching with water, the organic phase was washed with a saturated brine solution and water, then dried with MgSO₄ and concentrated under vacuum. The resultant liquid was purified by GPC giving the desired 420 mg liquid **4** (50 %).

¹H NMR (400 MHz, 300K, CDCl₃) δ (ppm): 7.26 (s, 2H), 6.84 (s, 2H), 4.22 (t, *J* = 4.0, 4H), 3.87 – 3.79 (m, 4H), 3.76-3.71 (m, 4H), 3.62-3.56 (m, 4H), 3.40 (s, 6H), 0.35 (s, 18H). ¹³C NMR (300 K, 101 MHz, CDCl₃) δ(ppm): 154.98, 134.64, 128.05, 125.54, 116.15, 72.05, 71.41, 70.86, 70.01, 59.12.

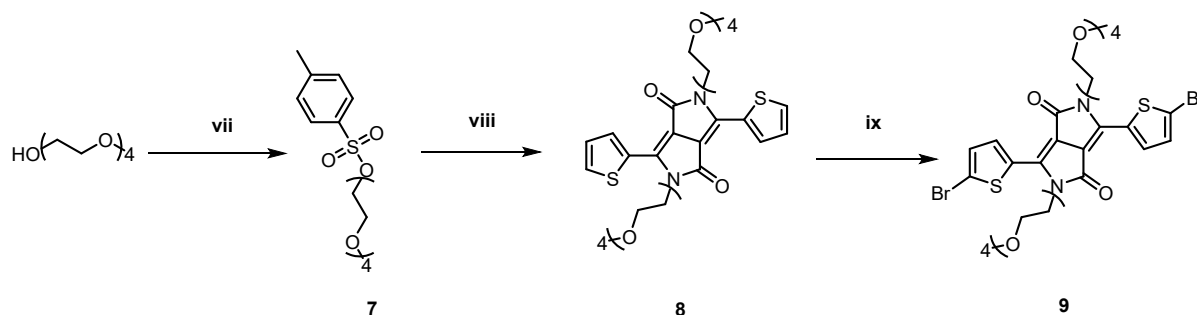
5: 2 (3.0 g, 10.67 mmol, 2.5 equiv.), 4,7-Bis(4,4,5,5-tetramethyl-1,3,2-dioxaborolan-2-yl)-2,1,3-benzothiadiazole (1.66 g, 4.28 mmol, 1 equiv.), one drop of tricaprylylmethylammonium chloride, Pd₂(dba)₃ (100 mg) and P(o-tol)₃ (200 mg) were added to round-bottom flask. After that, 10 mL aq. K₃PO₄ (2 M, degassed) and 20 mL toluene were added in one portion, and then stirred at 100 °C overnight and extracted by water and dried by anhydrous sodium sulfate. The solvent was removed under vacuum and purified by silica gel column chromatography to get 1.15 g **5** (50 %). ¹H NMR (300 K, 400 MHz, CDCl₃) δ (ppm): 8.44 (s, 2H), 7.37 (d, *J* = 5.6 Hz, 2H), 7.00 (d, *J* = 5.5 Hz, 2H), 4.34 (t, *J* = 4.0 Hz, 4H), 3.88 (t, *J* = 4.0 Hz, 4H), 3.72 – 3.64 (m, 4H), 3.58 – 3.48 (m, 4H), 3.37 (s, 6H). ¹³C NMR (300 K, 101 MHz, CDCl₃) δ: 155.21, 152.81,

127.55, 125.76, 124.10, 117.17, 116.84, 71.97, 71.05, 70.78, 69.94, 59.10. HRMS (ESI): m/z : calculated for $C_{24}H_{28}N_2O_6S_3$: 536.1109, $[M+1]^+$, found: 537.1180.

6: Under N_2 flow, a dry 100 mL round bottom flask with magnetic stir bar was charged with 500 mg **5** (0.93 mmol) and 20 mL dry THF. The solution was cooled to $-78\text{ }^\circ\text{C}$ with an acetone/dry ice bath over 15 min, and then 1.45 mL (1.6 M) *n*-butyllithium (2.33 mmol) was added dropwise over 10 min. The reaction mixture was allowed to stir at $-78\text{ }^\circ\text{C}$ for two hours, warmed to room temperature for 15 min, and then cooled back down to $-78\text{ }^\circ\text{C}$. 2.79 mL 1 M trimethyltin chloride in THF was added in one portion, and the reaction was stirred and allowed to warm to room temperature overnight. After quenching with water, the organic phase was washed with a saturated brine solution and water, then dried with $MgSO_4$ and concentrated under vacuum. The resultant liquid was purified by GPC giving the desired liquid 520 mg liquid (65 %).

1H NMR (300 K, 400 MHz, $CDCl_3$) δ (ppm): 8.38 (s, 2H), 7.06 (s, 2H), 4.39 – 4.31 (m, 4H), 3.93 – 3.84 (m, 4H), 3.72 – 3.67 (m, 4H), 3.57 – 3.51 (m, 4H), 3.37 (s, 6H), 0.42 (s, 18H). ^{13}C NMR (300 K, 101 MHz, $CDCl_3$) δ : 156.57, 139.03, 126.98, 124.61, 124.06, 122.56, 100.00, 71.99, 71.03, 70.79, 70.02, 59.12. HRMS (MALDI-TOF): m/z : calculated for $C_{30}H_{44}N_2O_6S_3Sn_2$: 864.0405, $[M+1]^+$, found: 865.0484.

Scheme S2. Synthetic route of 7-11.



Reaction conditions: vii) NaH, THF, $0\text{ }^\circ\text{C}$; viii) K_2CO_3 , tetrabutylammonium bromide, DMF, $100\text{ }^\circ\text{C}$; ix) NBS, $CHCl_3$, $0\text{ }^\circ\text{C}$.

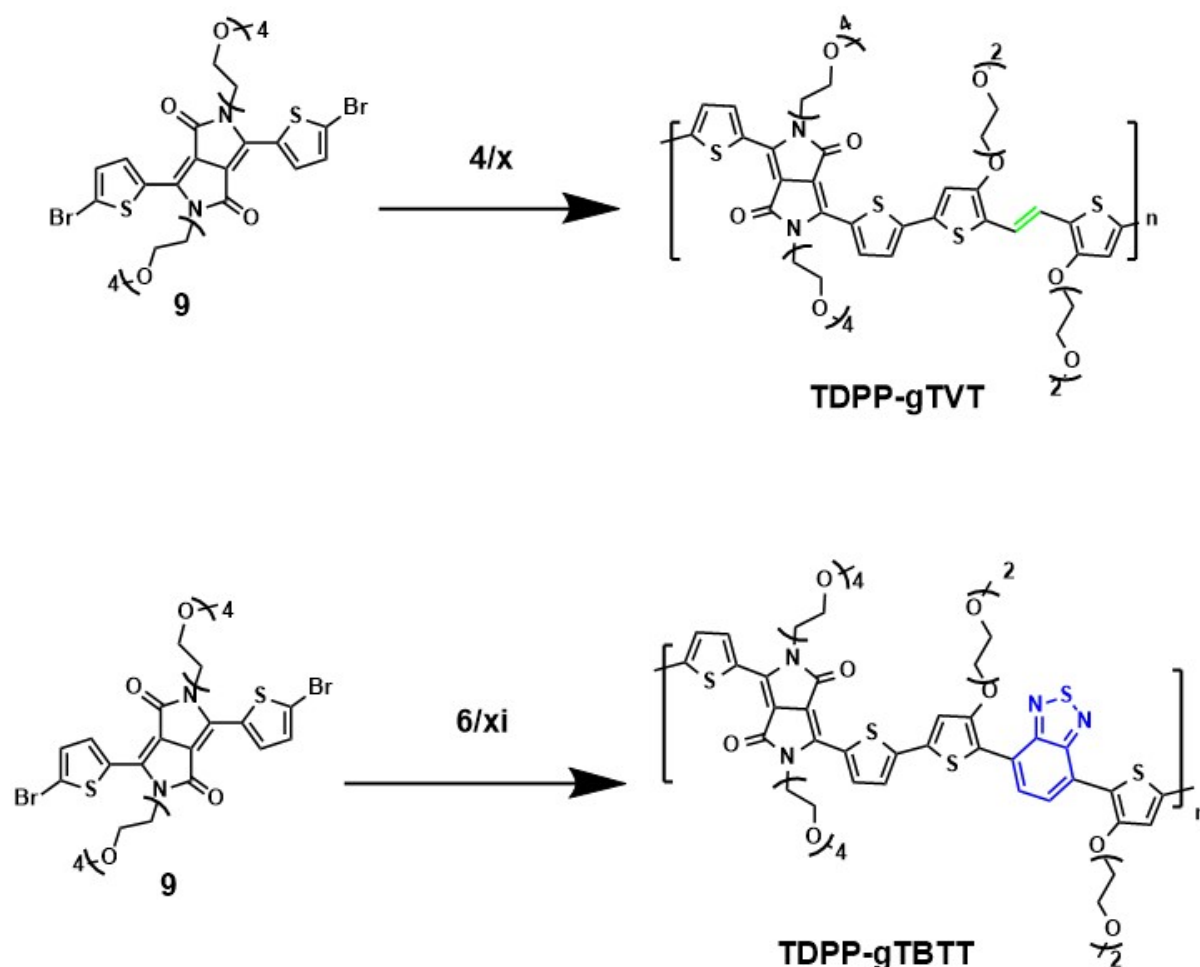
7-9 were synthesized according to the literature. [S2], [S13]

8: Thiophene-diketopyrrolopyrrole (3.00 g, 9.99 mmol), **7** (9.05 g, 24.98 mmol) potassium carbonate (4.14 g, 29.97 mmol) was mixed in a N_2 atmosphere. DMF (50 ml) and tetrabutylammonium bromide (1.61 g, 4.99 mmol) were added and reacted at room temperature $100\text{ }^\circ\text{C}$ for 5 h. DMF was removed under vacuum. The residue was purified by silica gel column chromatography to give 3.40 g (50%) compound **8**. 1H NMR (300 K, 400 MHz, CD_2Cl_2) δ (ppm): 8.73 (dd, $J = 3.9, 1.2$ Hz, 2H), 7.66 (dd, $J = 5.0, 1.1$ Hz, 2H), 7.26 (dd, $J = 5.0, 3.9$ Hz, 2H), 4.22 (t, $J = 6.3$ Hz, 4H), 3.72 (t, $J = 6.3$ Hz, 4H), 3.57 – 3.44 (m, 24H), 3.29 (s, 6H). ^{13}C NMR (300 K, 126 MHz, $CDCl_3$) δ : 161.54, 140.43, 134.78, 130.89, 129.67, 128.45, 107.88,

71.92, 70.60, 70.50, 68.94, 59.02, 41.87. HRMS (ESI): m/z : calculated for $C_{32}H_{44}N_2O_{10}S_2$: 680.2437, $[M+1]^+$, found: 681.2505.

9: 8 (0.68 g, 1.00 mmol) was taken in freshly distilled dry $CHCl_3$ (20 mL). bromosuccinimide (0.36 g, 2.01mmol) was added slowly portion wise for over 10 minutes at $0^\circ C$. The reaction mixture was stirred at the same temperature for 1 hour and kept at room temperature for 48 hours. Completion of the reaction was confirmed by TLC. Water was added to the crude mixture and extracted with CH_2Cl_2 (3 x 50 ml), washed with brine. The combined organic layers were collected and dried over anhydrous $MgSO_4$. The crude solid obtained was precipitated in methanol to give a pure product as purple solid 670 mg **9** (80 %). 1H NMR (300 K, 400 MHz, $CDCl_3$) δ (ppm): 8.47 (d, $J = 4.2$ Hz, 2H), 7.19 (d, $J = 4.2$ Hz, 2H), 4.15 (t, $J = 5.5$ Hz, 4H), 3.75 (t, $J = 5.6$ Hz, 4H), 3.63 – 3.50 (m, 24H), 3.35 (s, 6H). ^{13}C NMR (300 K, 101 MHz, $CDCl_3$) δ 161.37, 139.59, 134.95, 131.51, 131.20, 119.45, 108.06, 72.00, 70.85, 70.70, 70.60, 69.04, 59.14, 42.35. HRMS (ESI): m/z : calculated for $C_{32}H_{42}Br_2N_2O_{10}S_2$: 836.0648, $[M+1]^+$, found: 837.0708.

Scheme S3. Synthetic route of the polymers.



Reaction conditions: x, xi: Pd₂(dba)₃, P(o-tol)₃, toluene, reflux.

TDPP-gTVT:

9 (100.00 mg, 0.119 mmol, 1 equiv.), **4** (89.75mg, 0.119 mmol, 1 equiv.), Pd₂(dba)₃ (2.00 mg) and P(o-tol)₃ (4.00 mg) were added to a microwave vial. The tube was sealed and flushed with argon, and then degassed toluene (1 mL) was added. The mixture was thoroughly degassed under argon, and then the argon inlet was removed. The tube was stirred at 110 °C for 24 h. After cooling to RT, the polymer was precipitated into methanol, and filtered through a Soxhlet thimble. The polymer was extracted using Soxhlet apparatus with methanol, acetone, hexane, and chloroform. The chloroform solution was concentrated and precipitated into methanol. The precipitate was filtered and dried under vacuum to afford **TDPP-gTVT** (99.77 mg, 75 %), ¹H NMR (1,1,2,2-tetrachloroethane-d₂, 393K, 500 MHz), δ (ppm): 8.98-8.56 (broad), 7.45-6.68 (m), 4.27 (s), 4.01-3.32 (m).

TDPP-gTBTT:

9 (100.00 mg, 0.119 mmol, 1 equiv.), **6** (102.82 mg, 0.119 mmol, 1 equiv.), Pd₂(dba)₃ (2.00 mg) and P(o-tol)₃ (4.00 mg) were added to a microwave vial. The tube was sealed and flushed with argon, and then degassed toluene (1 mL) was added. The mixture was thoroughly degassed under argon, and then the argon inlet was removed. The tube was stirred at 110 °C for 24 h. After cooling to RT, the polymer was precipitated into methanol, and filtered through a Soxhlet thimble. The polymer was extracted using Soxhlet apparatus with methanol, acetone, hexane, and chloroform. The chloroform solution was concentrated and precipitated into methanol. The precipitate was filtered and dried under vacuum to afford **TDPP-gTBTT** (122.76 mg, 85 %), ¹H NMR (1,1,2,2-tetrachloroethane-d₂, 393K, 500 MHz), δ (ppm): 8.89-8.30 (m), 7.64-6.96(m), 4.5-4.17 (m), 4.12-3.22 (m).

12. NMR figures.

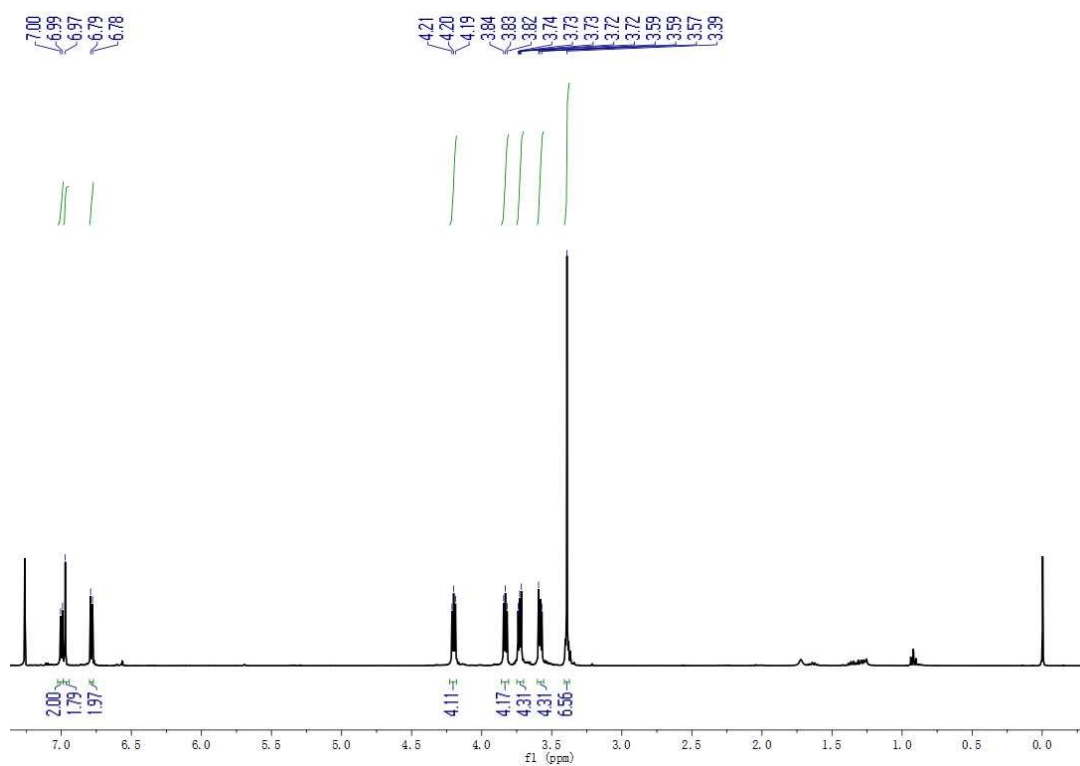


Figure S13: ¹H NMR of 3.

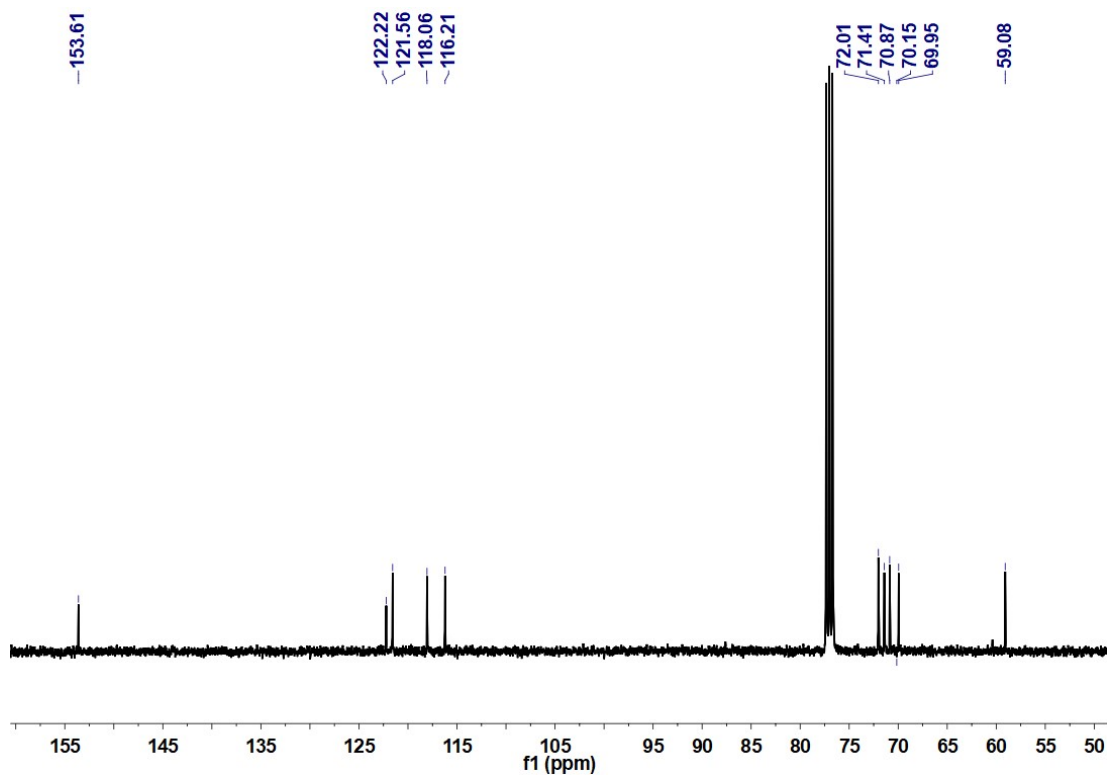


Figure S14: ^{13}C NMR of 3.

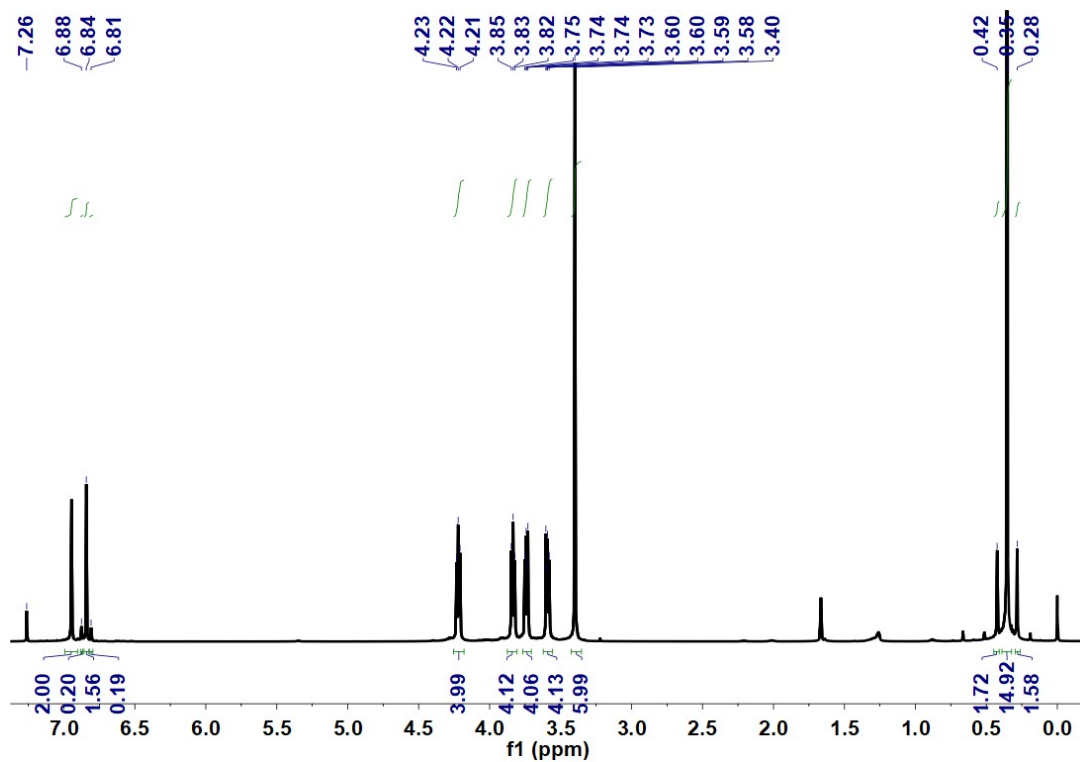


Figure S15: ^1H NMR of 4.

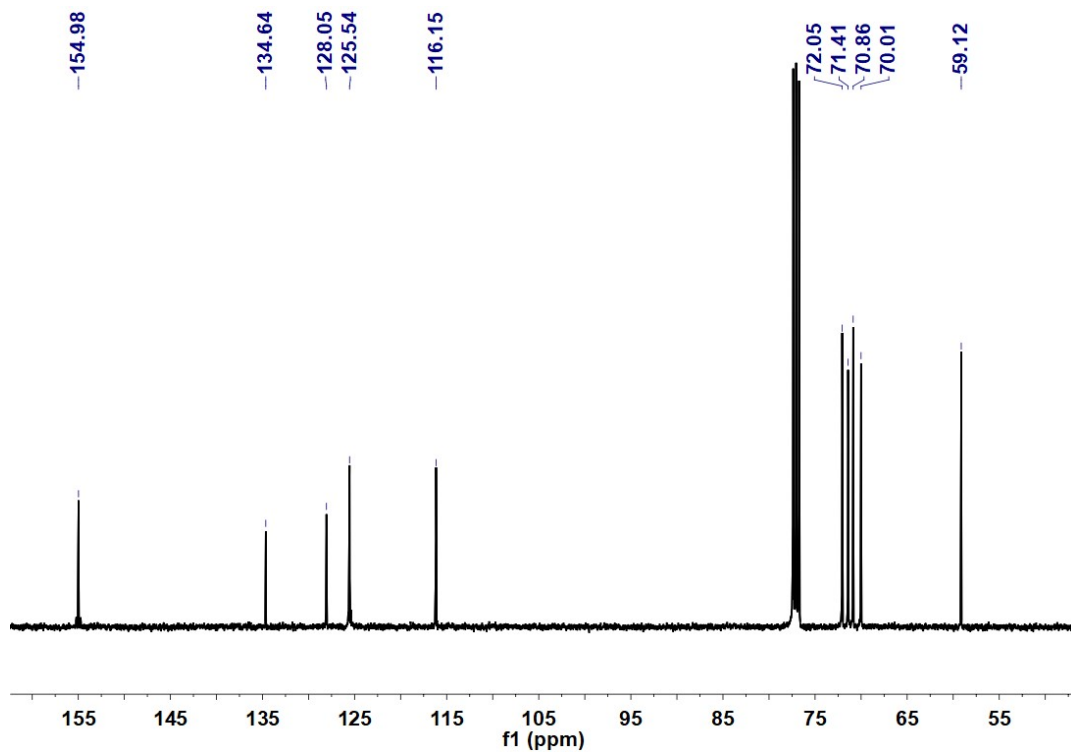


Figure S16: ^{13}C NMR spectrum of 4.

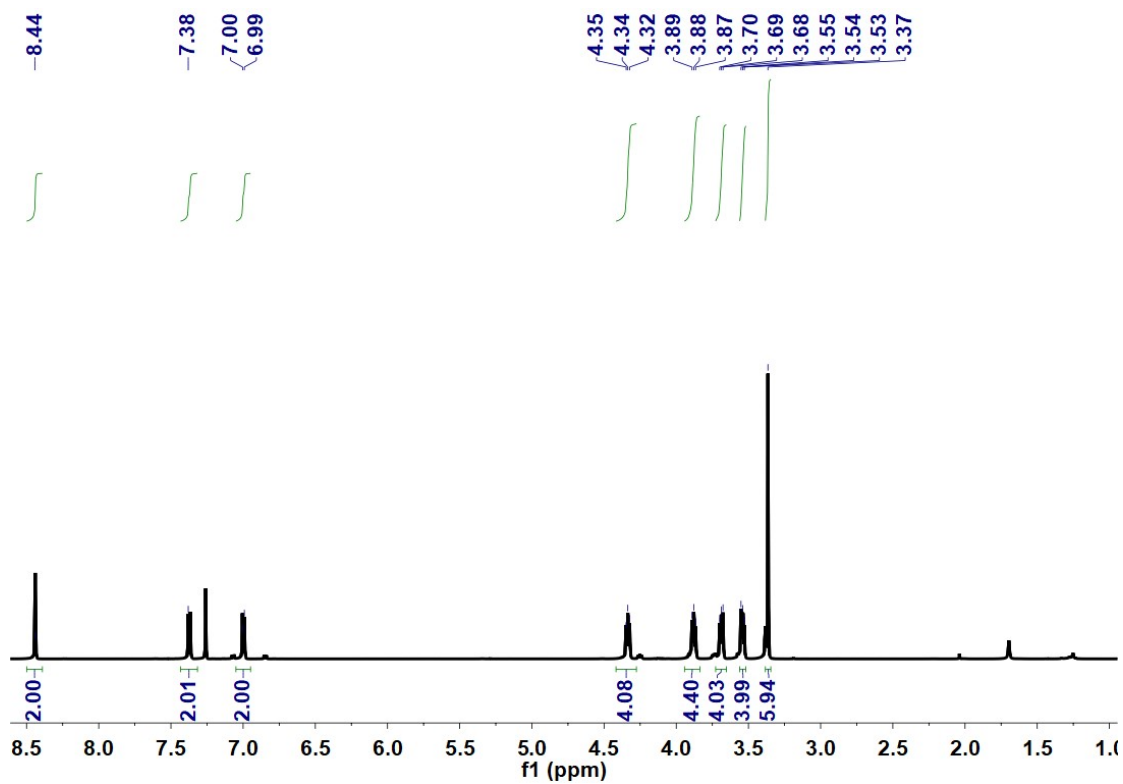


Figure S17: ^1H NMR of **5**.

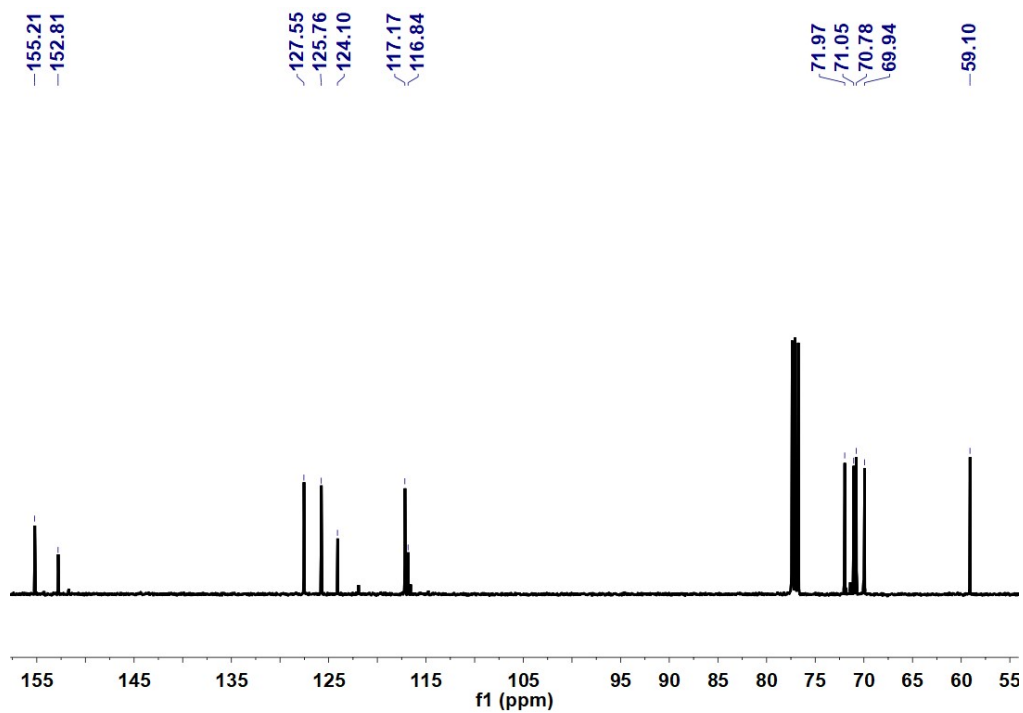


Figure S18: ^{13}C NMR of **5**.

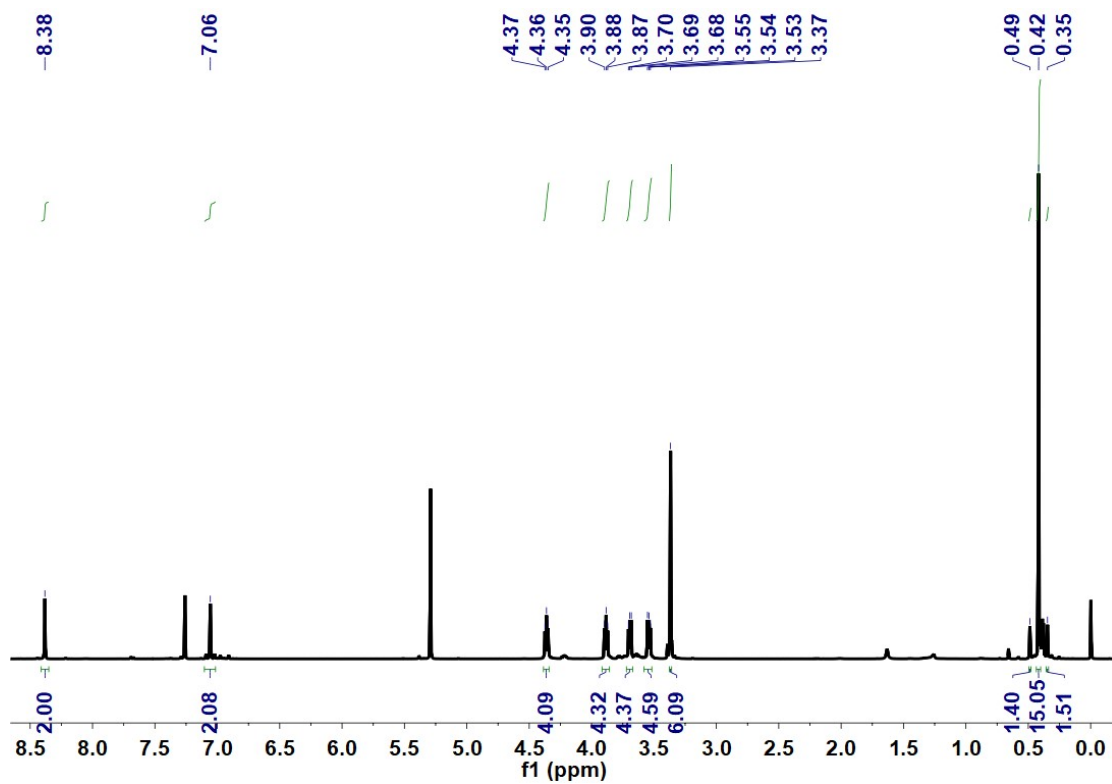


Figure S19: ^1H NMR of **6**.

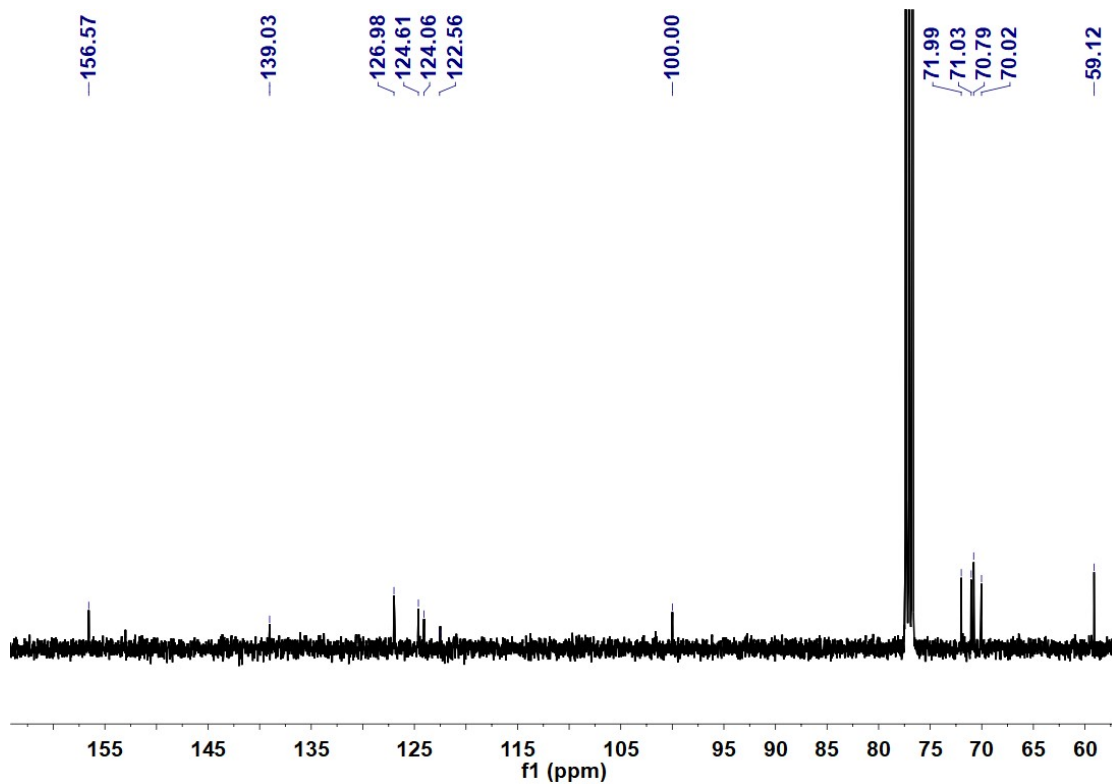


Figure S20: ^{13}C NMR of **6**.

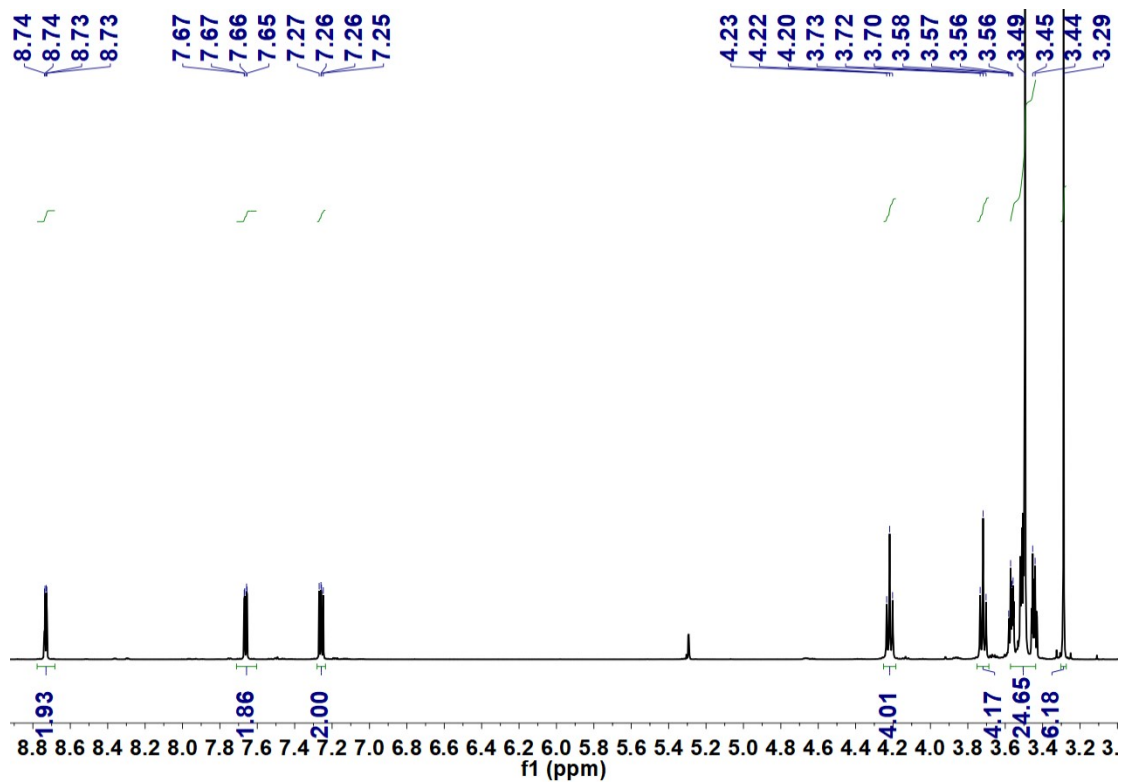


Figure S21: ^1H NMR spectrum of **8**.

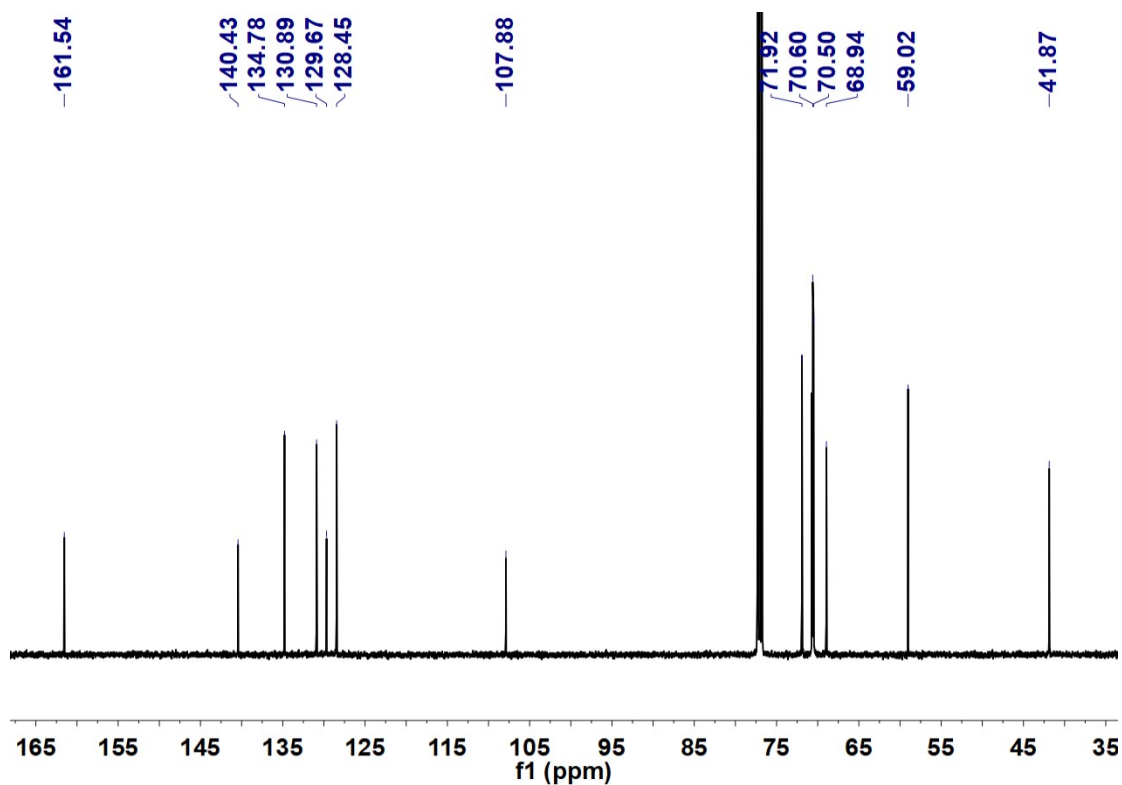


Figure S22: ^{13}C NMR spectrum of **8**.

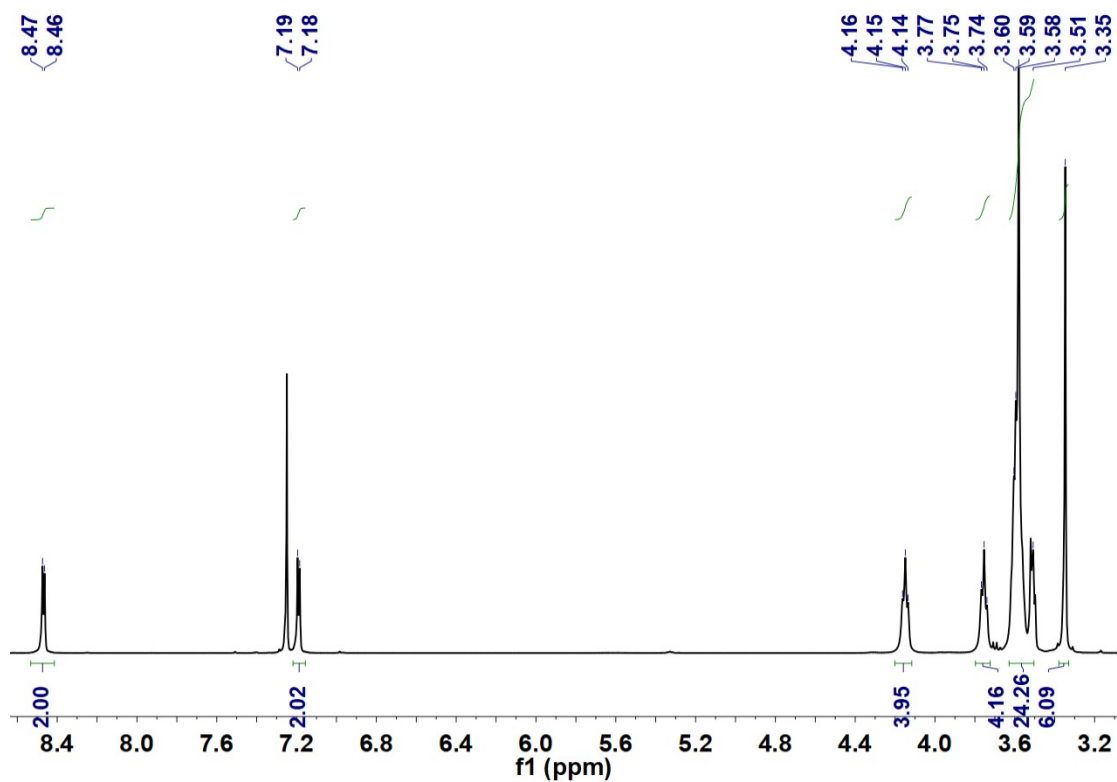


Figure S23: ¹H NMR spectrum of 9.

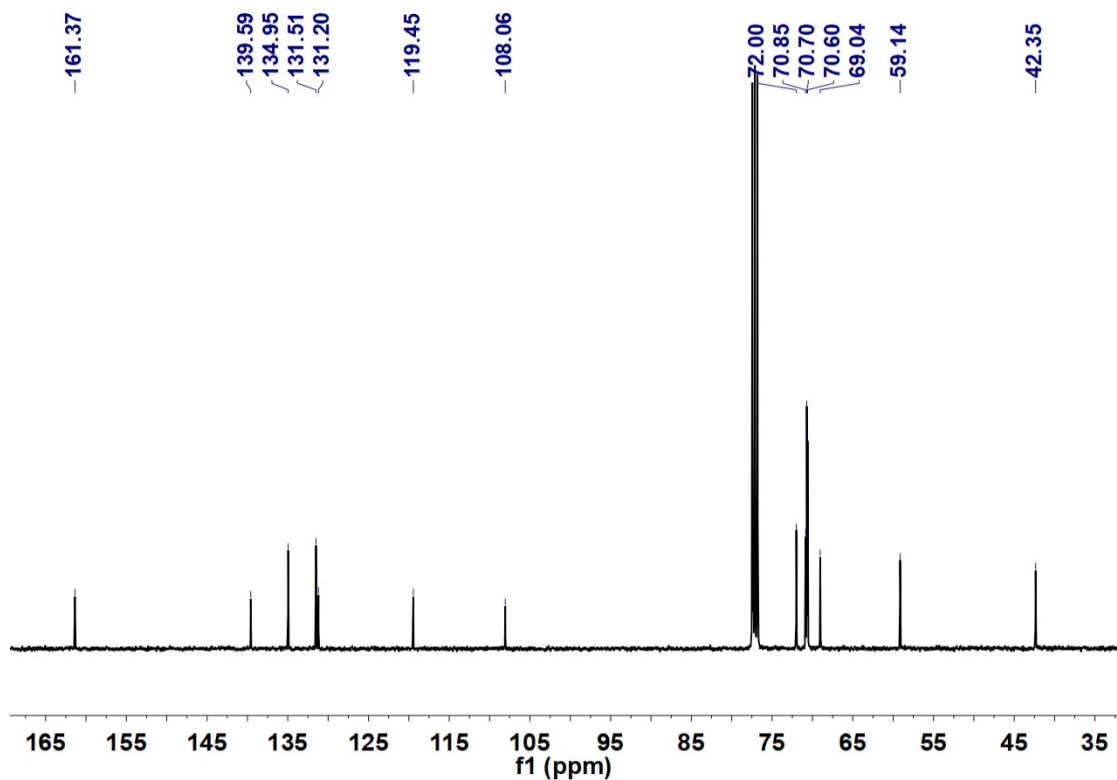


Figure S24: ¹³C NMR spectrum of 9.

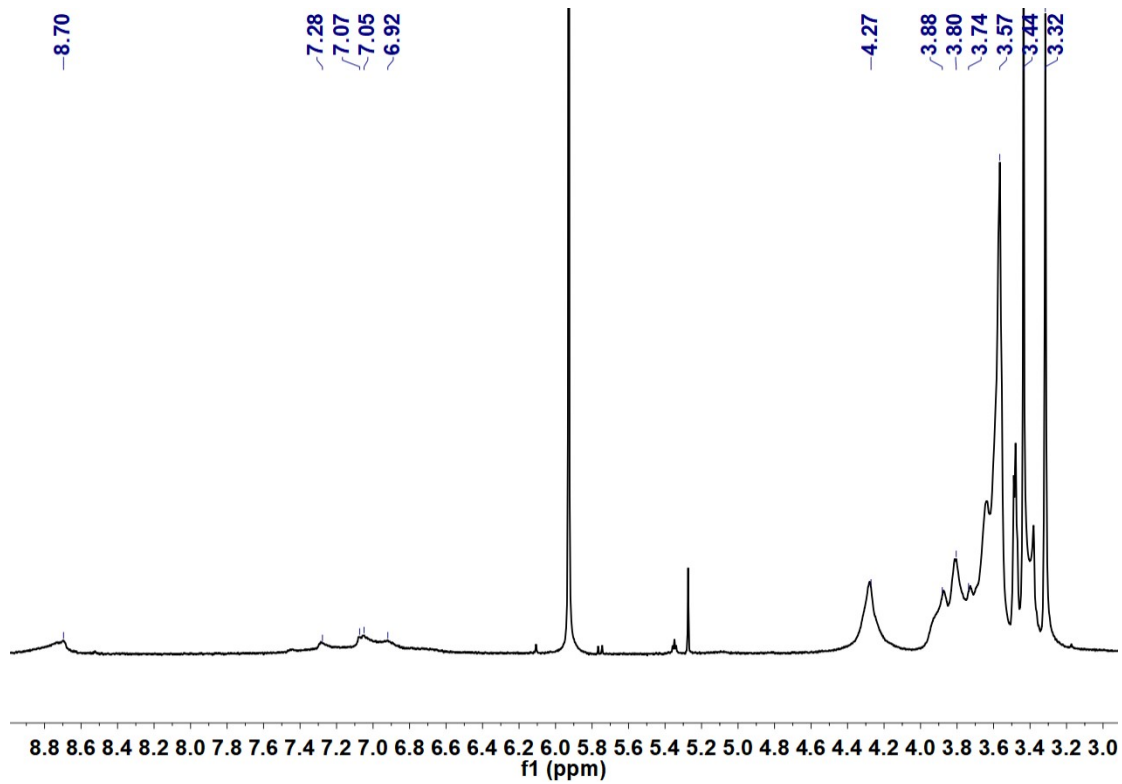


Figure S25: ^1H NMR spectrum of TDPP-gTVT.

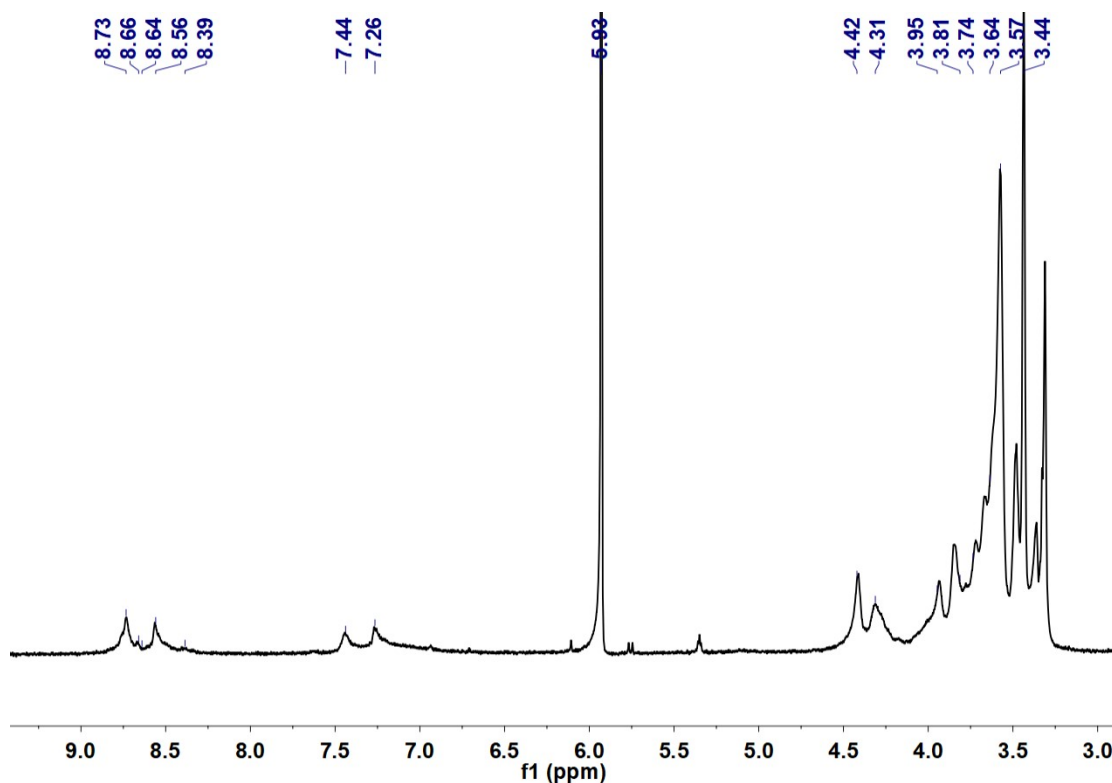


Figure S26: ^1H NMR spectrum of TDPP-gTBTT.

15. References

- [S1] A. Savva, C. Cendra, A. Giugni, B. Torre, J. Surgailis, D. Ohayon, A. Giovannitti, I. McCulloch, E. D. Fabrizio, A. Salleo, J. Rivnay, S. Inal, *Chem. Mater.*, 2019, **31**, 927- 937.
- [S2] Y. Wang, E. Zeglio, H. Liao, J. Xu, F. Liu, Z. Li, I. P. Maria, D. Mawad, A. Herland, I. McCulloch, W. Yue, *Chem. Mater.*, 2019, **31**, 9797-9806.
- [S3] A. T. Lill, D. X. Cao, M. Schrock, J. Vollbrecht, J. Huang, T. Nguyen-Dang, Brus, V. V. B. Yurash, D. Leifert, G. C. Bazan, T. Nguyen, *Adv. Mater.*, 2020, **32**, 1908120-1908129.
- [S4] A. Giovannitti, R. B. Rashid, Q. Thiburce, B. D. Paulsen, C. Cendra, K. Thorley, D. Moia, J. T. Mefford, D. Hanif, D. Weiyuan, M. Moser, A. Salleo, J. Nelson, I. McCulloch, J. Rivnay. *Adv. Mater.*, 2020, **32**, 1908047-1908055.
- [S5] M. Moser, A. Savva, K. Thorley, B.D. Paulsen, T. C. Hidalgo, D. Ohayon, H. Chen, A. Giovannitti, A. Marks, N. Gasparini, A. Wadsworth, J. Rivnay, S. Inal, I. McCulloch, *Angew. Chem. Int. Ed.*, 2021, **60**, 7777-7785
- [S6] X. Wu, Q. Liu, A. Surendran, S. E. Bottle, P. Sonar, W. L. Leong, *Adv. Electron. Mater.*, 2020, 2000701-2000708.
- [S7] C. B. Nielsen, A. Giovannitti, D. T. Sbircea, E. Bandiello, M. R. Niazi, D. A. Hanifi, M. Sessolo, A. Amassian, G. G. Malliaras, J. Rivnay, I. McCulloch, *J. Am. Chem. Soc.*, 2016, **138**, 10252.

-
- [S8] J. Qian, D. Wu, P. Cai, J. Xia, *Spectrochimica Acta Part A: Molecular and Biomolecular Spectroscopy*, 2019, **218**, 76-78.
- [S9] T. Yamamoto, K. Hisashi Kokubo, N. Nakamura, *Bull. Chem. Soc. Jpn.*, 2011, **84**, 1291-1293.
- [S10] H. Chen, Y. Guo, G. Yu, Y. Zhao, J. Zhang, D. Gao, H. Liu, Y. Liu, *Adv. Mater.*, 2012, **24**, 4618-4622.
- [S11] J. Lawrence, E. Goto, J. M. Ren, B. McDearmon, D. S. Kim, Y. P. G. Ochiai, C. D. Laitar, T. Higashihara, D. J. Hawker, *J. Am. Chem. Soc.*, 2017, **139**, 13735-13739.
- [S12] T. Matsumoto, K. Tanaka, Y. Chujo, *Macromolecules*, 2015, **48**, 1343-1351.
- [S13] C. Kanimozhi, N. Yaacobi-Gross, K. W. Chou, A. Amassian, T. W. Anthopoulos, S. Patil, *J. Am. Chem. Soc.*, 2012, **134**, 16532-16535.